# Supplementary Information

# Development of Rigidity-Controlled Terpolymer Donors for High-Performance and Mechanically Robust Organic Solar Cells

*Jinseck Kim,*[†,a] *Geon-U Kim,*[†,a] *Dong Jun Kim,*[†,b] *Seungjin Lee,*[a] *Dahyun Jeong,*[a] *Soodeok Seo,*[a] *Seo-Jin Ko**[,c], *Sung Cheol Yoon**[,c], *Taek-Soo Kim**[,b], *and Bumjoon J. Kim**[,a]

[a]Department of Chemical and Biomolecular Engineering, Korea Advanced Institute of Science and Technology (KAIST), Daejeon 34141, Republic of Korea

[*]Electronic mail: bumjoonkim@kaist.ac.kr

[b]Department of Mechanical Engineering, Korea Advanced Institute of Science and Technology (KAIST), Daejeon 34141, Republic of Korea

[*]Electronic mail: tskim1@kaist.ac.kr

[c]Division of Advanced Materials, Korea Research Institute of Chemical Technology (KRICT), Daejeon 34114, Republic of Korea

[*]Electronic mail: yoonsch@krict.re.kr; sjko927@krict.re.kr

# Table of Contents

and polar ($\gamma^p$) components in previous work.[6] All units are [mN $m^{-1}$].

- **Table S8**. Contact angles and surface tension of $P_D$s and Y6-BO, and the interfacial tension between $P_D$s and Y6-BO.
- **Table S9**. Mechanical properties of $P_D$ neat films and $P_D$:Y6-BO blend films.

## Experimental Section

### Materials

4,8-Bis(5-(2-ethylhexyl)-4-fluorothiophen-2-yl)benzo[1,2-*b*:4,5-*b*']dithiophene-2,6-diyl)bis(trimethylstannane) (FBDT-Sn), 2,6-dibromo-4,8-bis(5-(2-ethylhexyl)-4-fluoro thiophen-2-yl)benzo[1,2-*b*:4,5-*b*']dithiophene (FBDT-Br) and 1,3-bis(5-bromo thiophen-2-yl)-5,7-bis(2-ethylhexyl)benzo[1,2-*c*:4,5-*c*']dithiophene-4,8-dione (DTBDD-Br) were purchased from SunaTech Inc. and used without purification. 4,5-Bis(5-hexylthiophen-2-yl)benzene-1,2-diamine was synthesized by following previous literature.[1] Tetrakis(triphenylphosphine) palladium(0) ($Pd(PPh_3)_4$), anhydrous toluene, and *N*,*N*-dimethylformamide (DMF) were purchased from Sigma-Aldrich Inc.. 2,2'-((2Z,2'Z)-((12,13-Bis(2-butyloctyl)-3,9-diundecyl-12,13-dihydro-[1,2,5]thiadiazolo[3,4-*e*]thieno[2",3":4',5'] thieno[2',3':4,5] pyrrolo[3,2-*g*]thieno[2',3':4,5]thieno[3,2-*b*]indole-2,10-diyl)bis (methanyly lidene))bis(5,6-difluoro-3-oxo-2,3-dihydro-1*H*-indene-2,1-diylidene)) dimalononitrile (Y6-BO) was purchased from Derthon Inc.. 2,9-Bis(3-((3-(dimethylamino)propyl)amino)propyl) anthra[2,1,9-*def*:6,5,10-*d*'*e*'*f*']diisoquinoline-1,3,8,10 (2*H*,9*H*)-tetraone (PDINN) was synthesized *via* following previous report.[2]

### Synthesis

#### 1,4-Dibromo-7,8-bis(5-hexylthiophen-2-yl)-11H-benzo[4,5]imidazo[2,1-*a*]isoindol-11-one (BID-Br)

In a 100 mL round-bottom flask, 4,5-bis(5-hexylthiophen-2-yl)benzene-1,2-diamine (0.600 g, 1.36 mmol) and 3,6-dibromophthalic anhydride (0.416 g, 1.36 mmol) were added, and the flask was purged with nitrogen. Then, glacial acetic acid (8 mL) was added and flask was stirred at 130 ℃ for 5 h. After cooling to 25 ℃, the mixture was filtered and washed with water and methanol. After mixture was dried for 24 h, acetic anhydride (10 mL) was added,

and refluxed for 5 h under nitrogen atmosphere. After cooling to 25 ℃, the mixture was evaporated under reduced pressure, and crude product was purified by column chromatography yielding orange colored solid (yield: 42%). $^{1}$H NMR (400 MHz, $CDCl_3$) δ = 7.89 (d, J = 2.3 Hz, 2H), 7.59 (d, J = 8.6 Hz, 1H), 7.48 (d, J = 8.6 Hz, 1H), 6.76 (d, J = 3.5 Hz, 1H), 6.72 (d, J = 3.5 Hz, 1H), 6.64 (m, 2H), 2.85 – 2.71 (m, 4H), 1.71 – 1.60 (m, 4H), 1.44 – 1.23 (m, 12H), 0.90 (t, J = 6.8 Hz, 6H). $^{13}$C NMR (100 MHz, CDCl3): δ (ppm) = 157.3, 154.0, 148.4, 147.6, 147.1, 139.6, 139.5, 139.4, 137.3, 134.0, 133.9, 133.7, 132.3, 128.8. 127.4, 127.1, 124.0, 124.0, 123.9, 120.1, 116.2, 114.5, 31.6, 31.6, 30.1, 28.7, 22.6, 14.1. HR-MS: calculated for $C_{34}H_{34}Br_2N_2OS_2$ 708.0479, found 708.0499. Elemental analysis (%) calculated for C 57.47, H 4.82, N 3.94, S 9.02; found: C 57.38, H 4.85, N 4.01, S 8.89.

**Polymerization of polymer donors (*P*$_{D}$s)**

*P*$_{D}$s were polymerized *via* a modified procedure of previous liturature.[3] In a 20 mL reaction vial with FBDT-Sn (100 μmol), $Pd(PPh_3)_4$ (3 μmol) and DTBDD-Br (100 μmol) for PM6 or a mixture of DTBDD-Br:BID-Br with various ratios (90 μmol:10 μmol for PM6-B10, 80 μmol:20 μmol for PM6-B20, 70 μmol:30 μmol for PM6-B30) were added and degassed with $N_2$. Then, toluene (12.5 mL) and DMF (2.5 mL) were added, and the vial was heated to 105 ℃ for 2 h. After cooling to 25 ℃, the crude product was precipitated in methanol (150 mL), and filtered into cellulose thimble. After that, sequential Soxhlet extraction was performed with methanol, acetone, hexane, and dichloromethane to remove the catalyst and oligomers. Then, undissolved polymer was taken out from the thimble, dissolved in chloroform (150 mL) with vigorous stirring at 65 ℃ for 1 h and filtered. After that, condensed under reduced pressure, re-precipitated in methanol (150 mL) and dried under vacuum for 24 h before use.

**Solar Cell Fabrications**

For the study, the normal-type organic solar cells (OSCs) were prepared with indium tin oxide (ITO)/poly(3,4-ethylenedioxythiophene):poly(styrenesulfonate) (PEDOT:PSS) /active layer/PDINN/Ag. First, ITO-coated glass substrates were treated by ultrasonication with deionized water, acetone, and isopropyl alcohol. Then, the ITO substrates were dried for 3 h in an oven (70 °C) at an ambient pressure, and then plasma treated for 10 min. Spin-coating of the PEDOT:PSS solution (Clevios, AI4083) was performed at 3500 rpm for 30 s onto the ITO substrates. Then, the film/substrate was annealed in the air for 10 min at 150 °C before transferring into an $N_2$-filled glovebox. For the active layer solutions, $P_D$s and Y6-BO were dissolved together in chloroform at 60 °C with an optimized condition ($P_D$: Y6-BO weight ratio = 1:1.2, total concentration = 12 mg $mL^{-1}$, and 1-chloronaphtalene 0.5 vol%). The solution was spin-coated onto the PEDOT:PSS/ITO substrate to form an active layer with the thickness of 100 − 110 nm. Then, the samples were annealed at 100 ℃ for 5 min and dried with high vacuum (< $10^{-6}$ torr) for 30 min. Next, PDINN in methanol (1 mg $ml^{-1}$) was spin-coated with the condition of 3000 rpm for 30 s. Finally, Ag (120 nm) was deposited under high vacuum (~$10^{-6}$ Torr) in an evaporation chamber. Optical microscopy (OM) was used to measure the exact photoactive area of the mask (0.04 $cm^2$). Keithley 2400 SMU instrument was used to measure the photovoltaic efficiency of the devices under an Air Mass 1.5 G solar simulator (100 mW $cm^{-2}$, solar simulator: K201 LAB55, McScience Inc.), satisfying the Class AAA, ASTM Standards. K801SK302 (McScience Inc.) was used as a standard silicon reference cell to calibrate the exact solar intensity. K3100 IQX instrument (McScience Inc.) was used to analyze the external quantum efficiency (EQE) spectra, equipped with a monochromator (Newport) and an optical chopper (MC 2000 Thorlabs).

**Characterizations**

$^{1}$H and $^{13}$C nuclear magnetic resonance (NMR) spectra of BID-Br were recorded at room temperature on a 400 MHz NMR (Bruker) instrument using chloroform-d as deuterium solvent. $^{1}$H NMR spectra of $P_D$s, FBDT-Br, DTBDD-Br, and BID-Br were obtained at 100 ºC on a 400 MHz AV HD NMR (Bruker) instrument using 1,2-dichlorobenze-d4 as deuterium solvent. The solvent peaks were suppressed to clearly observe the aliphatic region using lc1pngpps pulse sequence. The number average molecular weight ($M_n$), polydispersity index ($Đ$) of the $P_D$s were estimated by gel permeation chromatography (GPC) with 1,2,4-trichlorobenzene as eluent at 100 ℃. Temperature-dependent UV-Vis absorption measurement was conducted using each $P_D$ solution *o*-dichlorobenzene as solvent. Grazing-incidence X-ray scattering (GIXS) measurements were conducted at Pohang Accelerator Laboratory, Korea in beamline 9A. The coherence lengths ($L_c$s) of the neat and blend films were calculated by using the Scherrer equation. Resonant soft x-ray scattering (RSoXS) measurements were performed at beamline 11.0.1.2 in the Advanced Light Source (USA). $P_D$:Y6-BO blend films for the RSoXS measurement were prepared on a 100 nm-thick, 1.0 mm × 1.0 mm $Si_3N_4$ membrane supported by a 200-μm thick, 5 mm × 5 mm silicon frame (Norcada Inc.). The domain spacing is calculated from the equation of $2\pi q_{peak}^{-1}$ from the RSoXS profile. The relative domain purity was estimated as the relative ratio of square-root of the integrated scattering intensity in the $Iq^2$ vs. $q$ plot. The integration range in this study was $q$ = 0.0003 to 0.0100 Å$^{-1}$.

**Solubility test of $P_D$s**

The solubilities of the $P_D$s were evaluated in the chloroform at 60 ºC. The concentration of solutions was 30 mg mL$^{-1}$. After heating the solution at 60 ºC for 12 h, the solutions were filtered by a polytetrafluoroethylene (PVDF) membrane with a pore size of 5 μm

diameter. After filtration, the remaining solvent was completely evaporated and the weight of solid was measured to estimate solubilities of the $P_D$s. A filter with a smaller pore size of 0.45 μm diameter was also tested, but all the $P_D$ solutions were clogged.

**Space-charge-limited current (SCLC) mobility measurements**

SCLC method was introduced for measuring hole mobilities ($\mu_h$s) of neat $P_D$ films, and $\mu_h$ and electron mobility ($\mu_e$) of $P_D$s:Y6-BO blend films in a device structures of ITO/PEDOT:PSS/$P_D$s or $P_D$s:Y6-BO/Au (hole-only) and ITO/ZnO/$P_D$s:Y6-BO/PFN-Br/Al (electron-only). The charge mobilities can be calculated from Mott-Gurney law.

$$J = \frac{9\varepsilon_0\varepsilon_r\mu_0 V^2}{8L^3}$$

where $J$ is the current density, $\varepsilon_0$ is the permittivity of free space ($8.85 \times 10^{-14}$ F cm$^{-1}$), $\varepsilon_r$ is the relative dielectric constant of the active layer, $\mu_0$ is the hole or electron mobility, $V$ is the potential across the device ($V = V_{applied} - V_{bi} - V_r$, where $V_{bi}$ is the built-in potential and $V_r$ is the voltage drop caused by the resistance), and $L$ is the thickness of the neat or blend films. The measured film thicknesses of the films were in the range of 85 – 110 nm and voltage was applied for the current-voltage measurements in the range of 0 to 6 V. The charge mobilities can be calculated from the slope of the $J^{1/2}$-$V$ curves.

**Contact angle measurements and interfacial tension calculation**

Contact angles of the materials were measured by a contact angle analyzer (Phoenix 150, SEO, Korea). The surface tension of the thin films obtained from the Wu model, using both the contact angles from water and glycerol on pristine films.[4, 5] The detailed calculation method is described below.

$$\gamma_{\mathrm{water}}(1+\cos\theta_{\mathrm{water}}) = \frac{4\gamma^{\mathrm{d}}_{\mathrm{water}}\gamma^{\mathrm{d}}}{\gamma^{\mathrm{d}}_{\mathrm{water}}+\gamma^{\mathrm{d}}} + \frac{4\gamma^{\mathrm{p}}_{\mathrm{water}}\gamma^{\mathrm{p}}}{\gamma^{\mathrm{p}}_{\mathrm{water}}+\gamma^{\mathrm{p}}}$$

$$\gamma_{\mathrm{Glycerol}}\left(1+\cos\theta_{\mathrm{Glycerol}}\right) = \frac{4\gamma^{\mathrm{d}}_{\mathrm{Glycerol}}\gamma^{\mathrm{d}}}{\gamma^{\mathrm{d}}_{\mathrm{Glycerol}}+\gamma^{\mathrm{d}}} + \frac{4\gamma^{\mathrm{p}}_{\mathrm{Glycerol}}\gamma^{\mathrm{p}}}{\gamma^{\mathrm{p}}_{\mathrm{Glycerol}}+\gamma^{\mathrm{p}}}$$

$$\gamma^{\mathrm{total}} = \gamma^{\mathrm{d}} + \gamma^{\mathrm{p}}$$

Where $\gamma^{\mathrm{total}}$ is the total surface tension of the materials that comes from the sum of dispersion component $\gamma^{\mathrm{d}}$ and polar component $\gamma^{\mathrm{p}}$. Then, the interfacial tension ($\gamma^{\mathrm{D\text{-}A}}$, D = donor and A= acceptor) between donor and acceptor was calculated based on the surface tensions, following the calculation below.

$$\gamma^{\mathrm{Donor-Acceptor}} = \gamma^{\mathrm{Donor}} + \gamma^{\mathrm{Acceptor}} - \frac{4\gamma^{\mathrm{d}}_{\mathrm{Donor}}\gamma^{\mathrm{d}}_{\mathrm{Acceptor}}}{\gamma^{\mathrm{d}}_{\mathrm{Donor}}+\gamma^{\mathrm{d}}_{\mathrm{Acceptor}}} - \frac{4\gamma^{\mathrm{p}}_{\mathrm{Donor}}\gamma^{\mathrm{d}}_{\mathrm{Acceptor}}}{\gamma^{\mathrm{p}}_{\mathrm{Donor}}+\gamma^{\mathrm{d}}_{\mathrm{Acceptor}}}$$

**Pseudo-freestanding tensile test**

The blends films were prepared with the same conditions as those used for the OSC fabrications. The films were spin-casted onto polystyrene sulfonic acid-coated glass substrates, and cut into a dog-bone shape by a femtosecond laser. Then, the films were floated onto the water surface, and attached to the grips by van der Waals forces. The strain was applied at a fixed strain rate ($0.8 \times 10^{-3}$ $s^{-1}$), and the tensile load values were measured by a load cell with high resolution (LTS-10GA, KYOWA, Japan). Elastic modulus was calculated using the least square method for the slope of the linear region of the stress–strain curve within 0.5% strain. The crack-onset strain (COS) of a thin film was determined as the strain value that the tensile load starts to decrease rapidly by cracking.

## Supplementary Figures & Tables

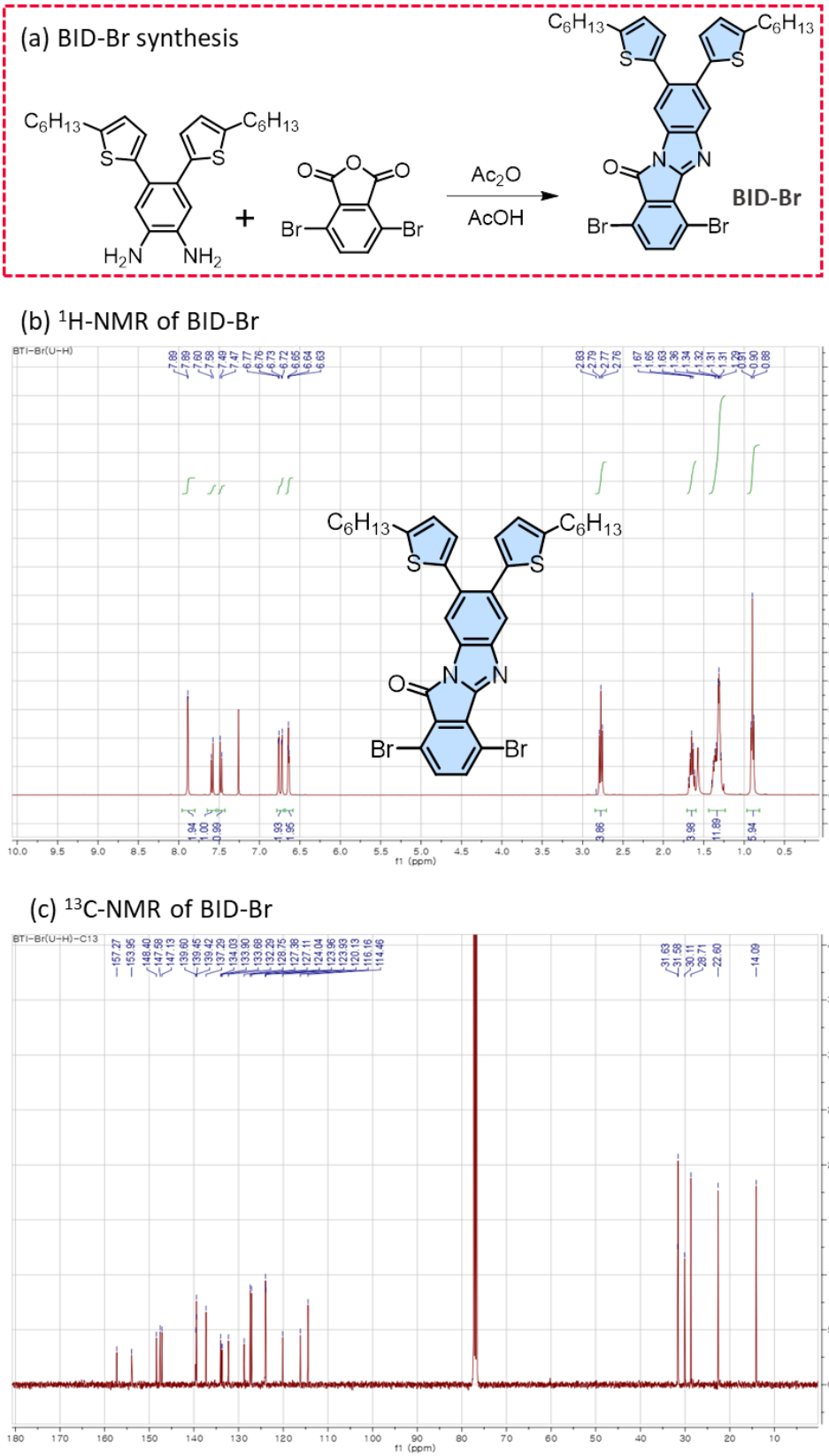


**Fig. S1.** a) Synthetic scheme, b) $^1$H-NMR and c) $^{13}$C-NMR spectra of BID-Br.

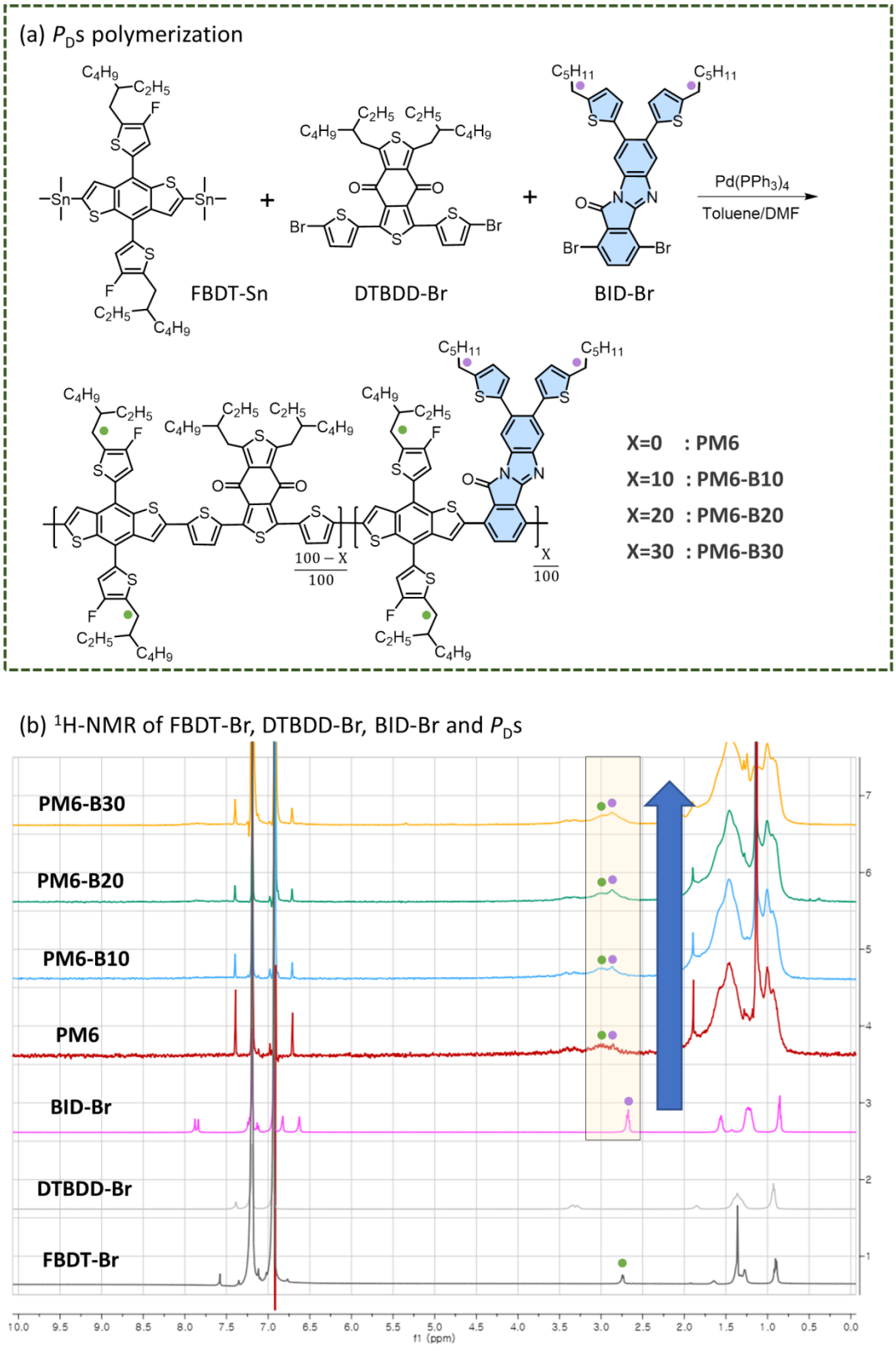


**Fig. S2**. a) Polymerization scheme and b) overlapped $^{1}$H-NMR spectra of brominated monomers and $P_D$s.

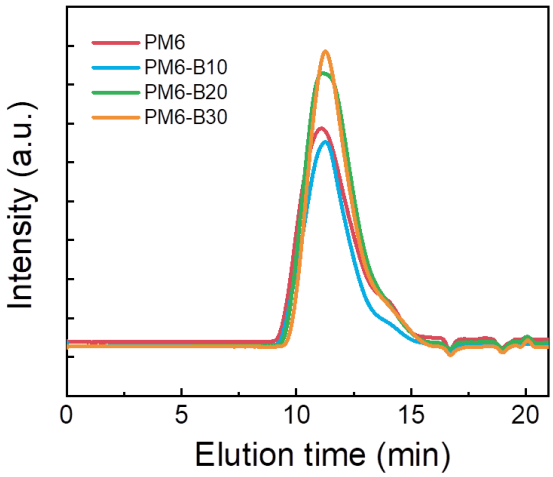


**Fig. S3.** GPC curves of $P_{DS}$.

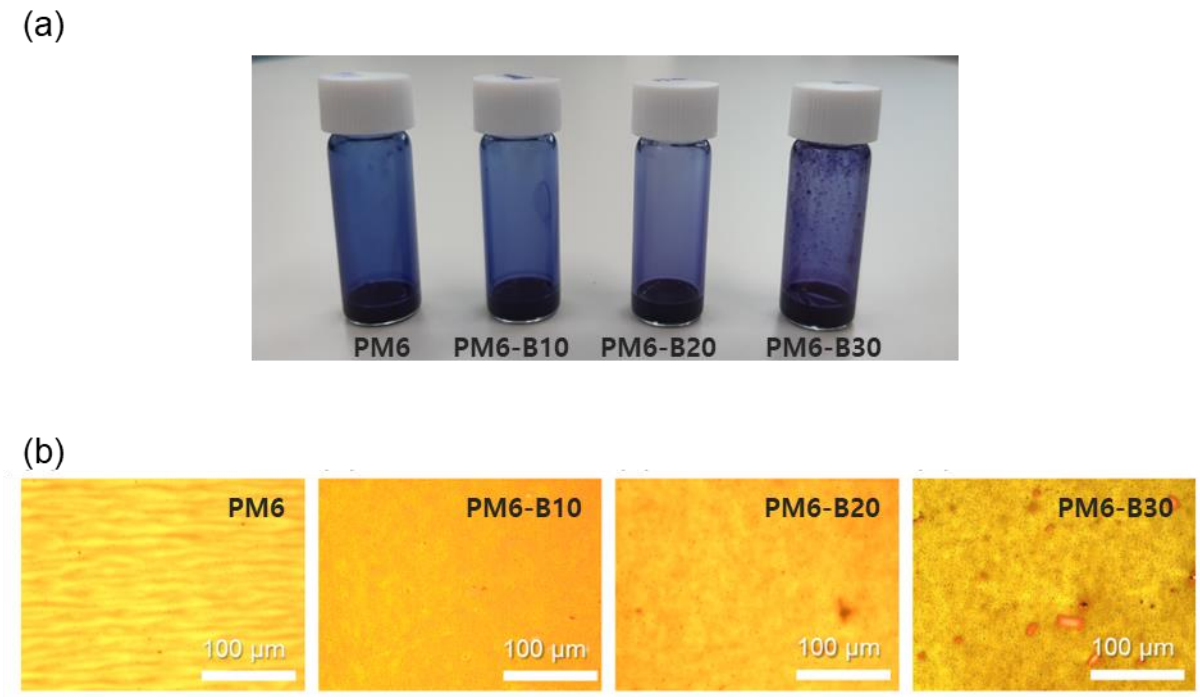


**Fig. S4.** a) Photo images of $P_D$ solutions in chloroform (5 mg mL$^{-1}$). Solutions were heated at 60 ºC for 12 h and, then, cooled to room temperature. b) OM images of $P_D$ neat films from the solutions.

**Table S1**. Solubilities of $P_D$s in chloroform.

| $P_D$s | Solubility [mg mL$^{-1}$] |
|---|---|
| PM6 | 20.2 |
| PM6-B10 | 23.0 |
| PM6-B20 | 16.6 |
| PM6-B30 | 2.8 |

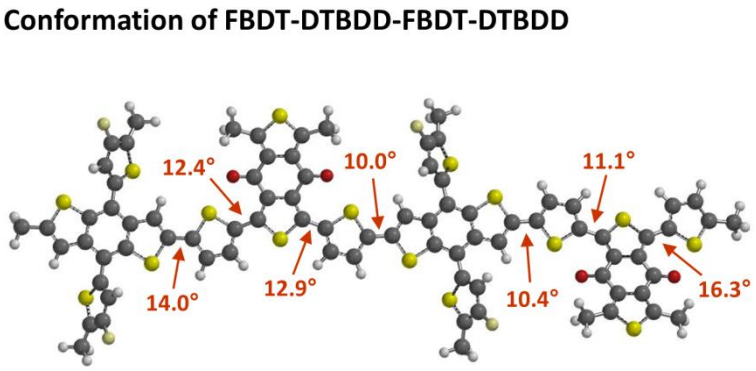


**Fig. S5.** Simulated molecular conformation of FBDT-DTBDD-FBDT-DTBDD.

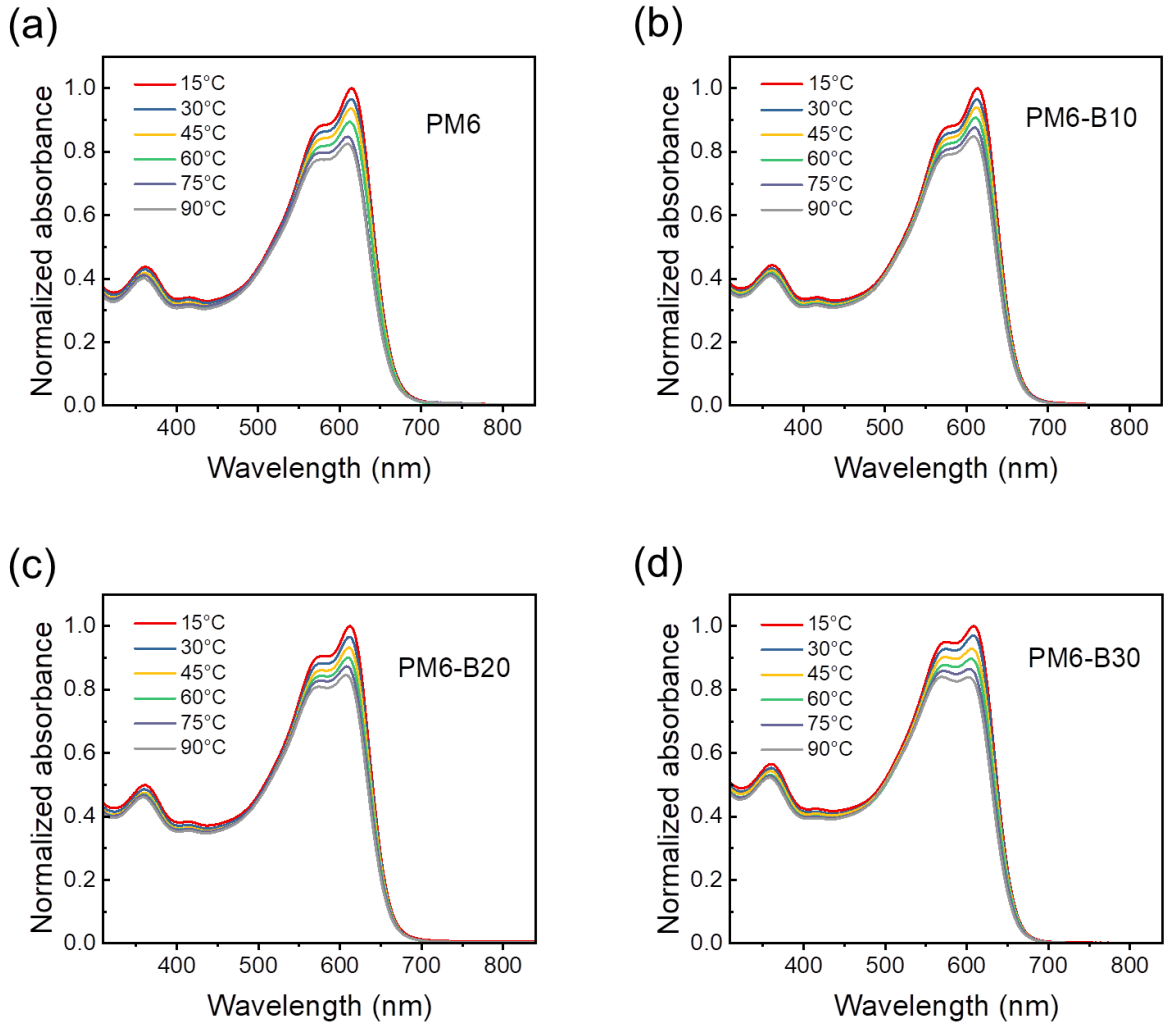


**Fig. S6.** Temperature-dependent UV-Vis absorption spectra of $P_{DS}$ in *o*-dichlorobenzene solvent.

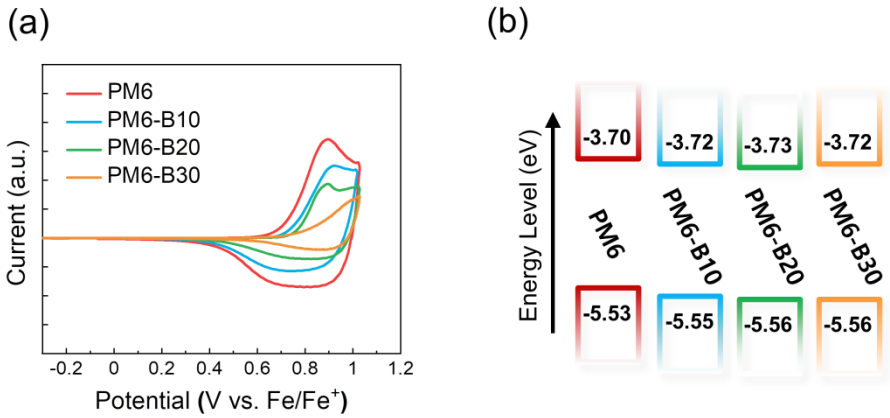


**Fig. S7.** a) Cyclic voltammetry curves of $P_D$s; b) energy levels of $P_D$s.

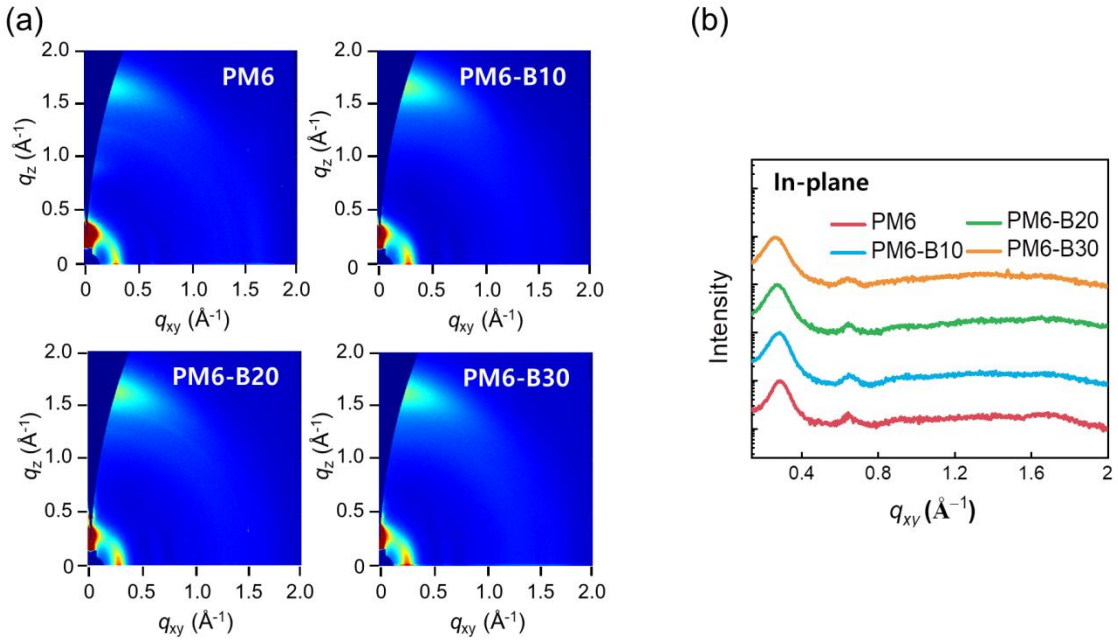


**Fig. S8.** GIXS a) 2D images and b) 1D linecut profiles of neat $P_D$ films.

**Table S2**. GIXS information of neat $P_D$ films.

| $P_{DS}$ | $d_{(100)}$ [Å] | $L_{c(100)}$ [Å] | $d_{(010)}$ [Å] | $L_{c(010)}$ [Å] |
|---|---|---|---|---|
| PM6 | 22.1 | 74.1 | 3.82 | 27.4 |
| PM6-B10 | 22.7 | 67.4 | 3.82 | 26.1 |
| PM6-B20 | 23.3 | 64.5 | 3.83 | 24.9 |
| PM6-B30 | 24.2 | 61.2 | 3.85 | 24.8 |

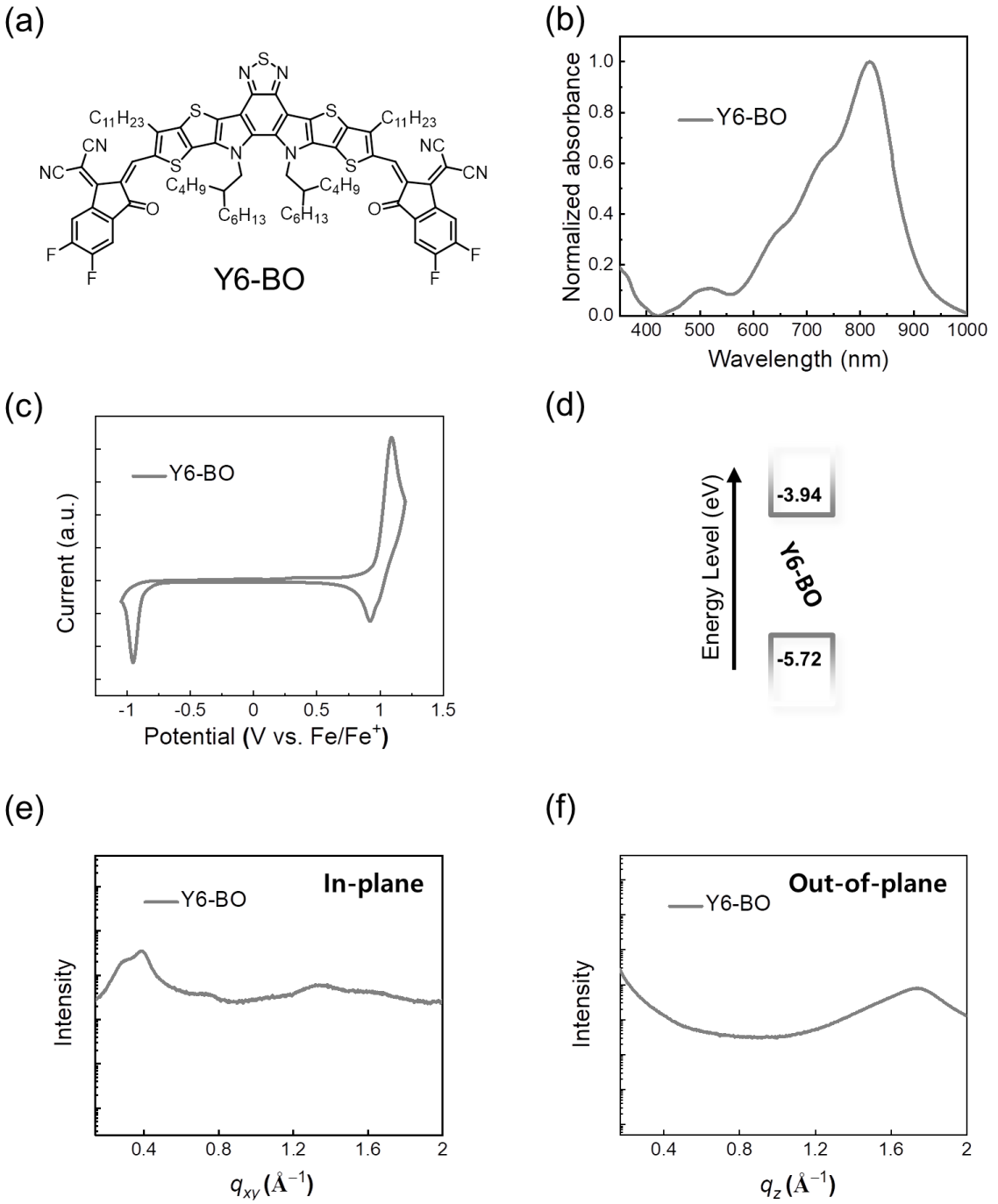


**Fig. S9**. a) Molecular structure of Y6-BO; b) UV-Vis absorption spectrum of Y6-BO in a film; c) cyclic voltammetry curve and d) energy levels of Y6-BO; GIXS linecut profiles of neat Y6-BO film: e) in-plane direction and f) out-of-plane direction.

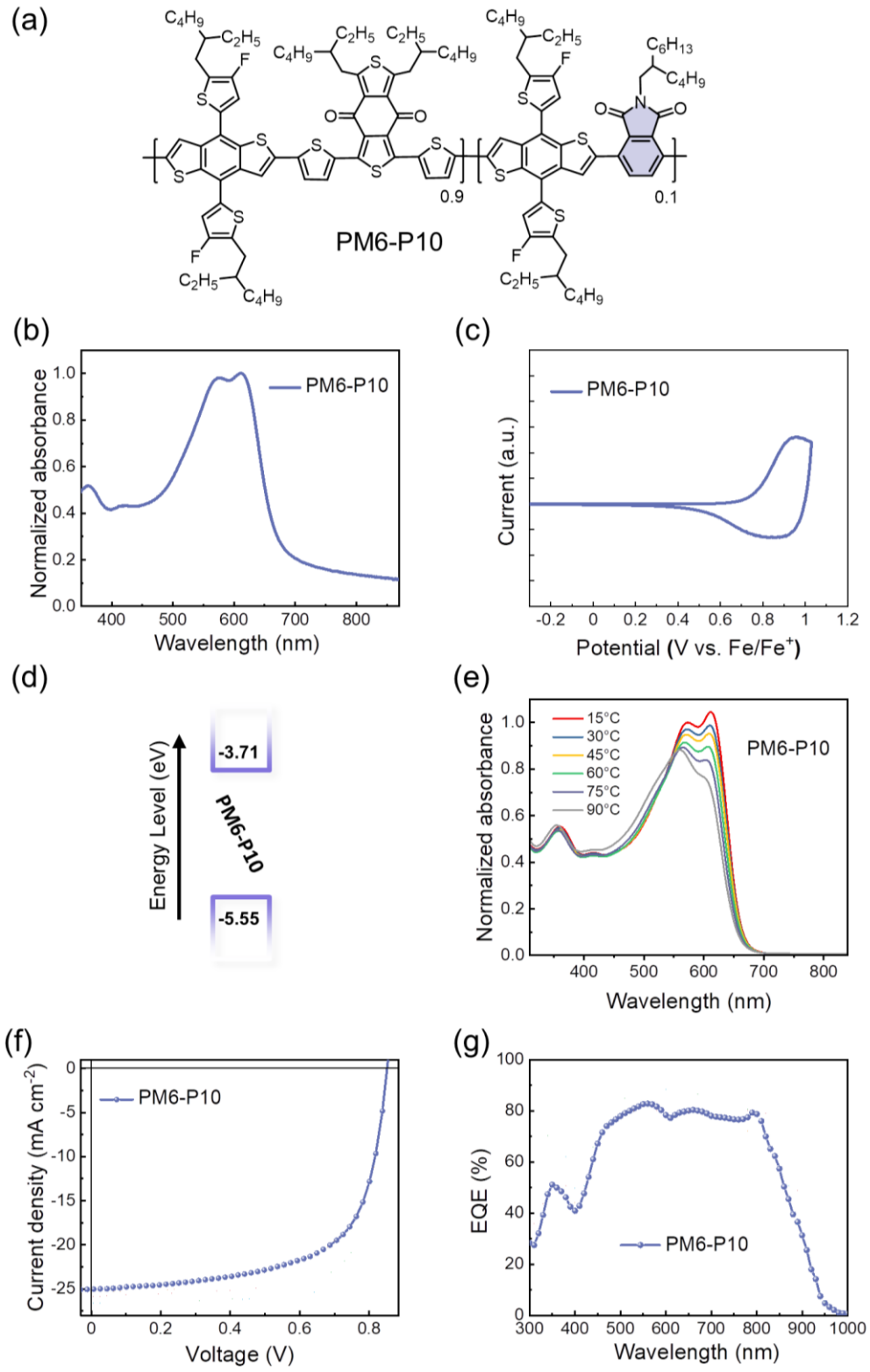


**Fig. S10**. a) Molecular structure of PM6-P10; b) UV-Vis absorption spectrum of PM6-P10 in film; c) cyclic voltammetry curve; d) energy levels and e) temperature-dependent UV-Vis absorption spectrum (in *o*-dichlorobenzene) of PM6-P10. Photovoltaic characteristics of PM6-P10:Y6-BO OSC; f) *J*-*V* curve and g) EQE spectrum.

**Table S3.** Material characteristics of PM6-P10.

| $P_{DS}$ | $M_n$ ($Đ$) [a)] [kg mol$^{-1}$] | $\lambda_{film}^{max}$ [b)] [nm] | $E_g^{opt}$ [b)] [eV] | $E_{HOMO}$ [c)] [eV] | $E_{LUMO}$ [d)] [eV] | $\mu_h^{SCLC}$ ($\times 10^{-4}$) [cm$^2$ V$^{-1}$ s$^{-1}$] |
|---|---|---|---|---|---|---|
| PM6-P10 | 131 (2.75) | 612 | 1.84 | -5.55 | -3.71 | 0.8 ± 0.2 |

[a)] Estimated by GPC with 1,2,4-trichlorobenzene as eluent. [b)] Evaluated from UV-Vis absorption spectrum in film. [c)] Measured from cyclic-voltammetry [d)] Calculated by using equation of $E_{LUMO} = E_{HOMO} + E_g^{opt}$.

**Table S4.** Photovoltaic performance of PM6-P10:Y6-BO OSC.

| $P_D$ | $V_{oc}$ [V] | $J_{sc}$ [mA cm$^{-2}$] | Calcd. $J_{sc}$ [a)] [mA cm$^{-2}$] | FF | $PCE_{max}$ ($PCE_{avg}$) [b)] [%] |
|---|---|---|---|---|---|
| PM6-P10 | 0.85 | 25.04 | 24.46 | 0.65 | 13.77 (13.30 ± 0.32) |

[a)] Calculated from the EQE spectrum. [b)] Average values based on at least 10 devices.

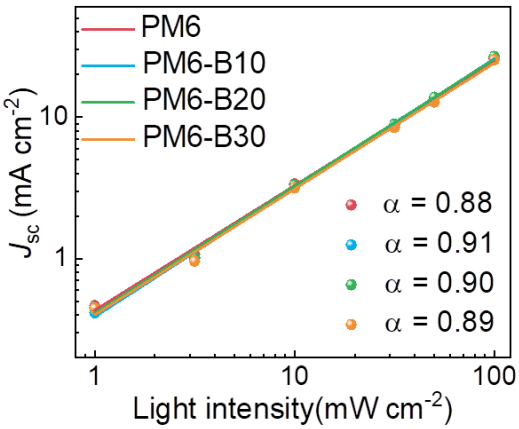


**Fig. S11**. Light intensity−dependent $J_{sc}$ of $P_D$:Y6-BO OSCs.

**Table S5**. SCLC mobilities of the $P_D$:Y6-BO blend films.

| $P_D$s | $\mu_e$ ($cm^2$ $V^{-1}$ $s^{-1}$) | $\mu_h$ ($cm^2$ $V^{-1}$ $s^{-1}$) | $\mu_e/\mu_h$ |
|---|---|---|---|
| PM6 | $(6.1 \pm 0.7) \times 10^{-4}$ | $(4.8 \pm 0.4) \times 10^{-4}$ | 1.3 |
| PM6-B10 | $(5.7 \pm 0.3) \times 10^{-4}$ | $(4.8 \pm 0.7) \times 10^{-4}$ | 1.2 |
| PM6-B20 | $(5.5 \pm 0.5) \times 10^{-4}$ | $(4.1 \pm 0.4) \times 10^{-4}$ | 1.3 |
| PM6-B30 | $(2.7 \pm 1.0) \times 10^{-4}$ | $(1.4 \pm 0.7) \times 10^{-4}$ | 1.9 |

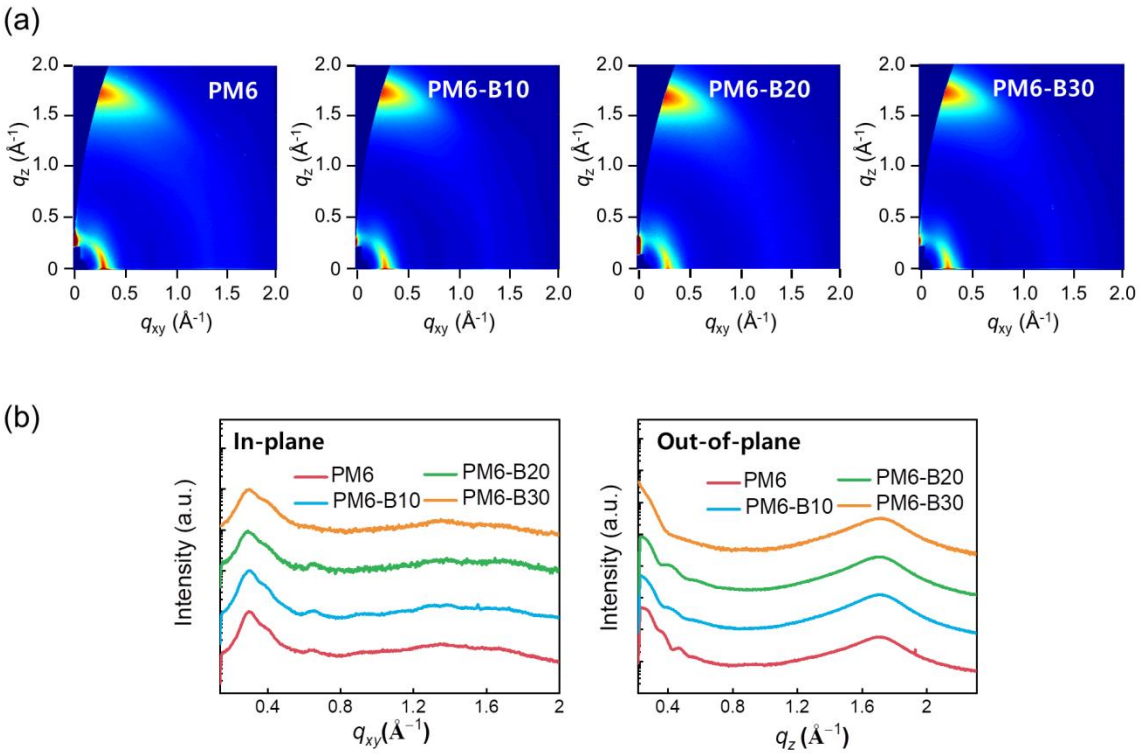


**Fig. S12.** GIXS a) 2D image and b) 1D linecut of $P_D$:Y6-BO blend films.

**Table S6**. GIXS information of $P_D$:Y6-BO blend films.

| $P_D$s | $d_{(100)}$ [Å] | $L_{c(100)}$ [Å] | $d_{(010)}$ [Å] | $L_{c(010)}$ [Å] |
|---|---|---|---|---|
| PM6 | 20.7 | 62.8 | 3.71 | 23.9 |
| PM6-B10 | 20.8 | 57.0 | 3.70 | 23.3 |
| PM6-B20 | 21.1 | 52.0 | 3.71 | 23.4 |
| PM6-B30 | 20.9 | 47.0 | 3.70 | 22.2 |

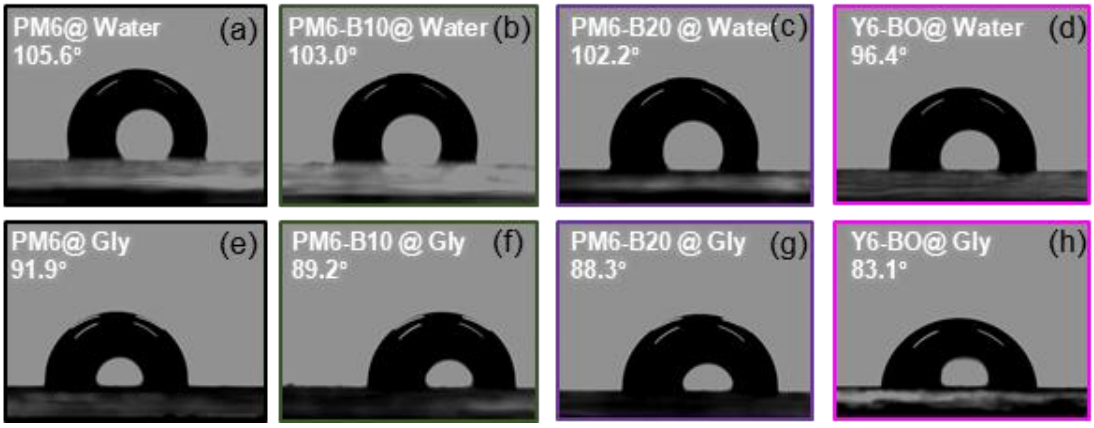


**Fig. S13.** Photo images of contact angle measurements with (a – d) water and (e – h) glycerol on $P_D$ and Y6-BO neat films.

**Table S7.** Surface tensions (γ) of solvents (water and glycerol) and their dispersive ($\gamma^d$) and polar ($\gamma^p$) components in previous work.[6] All units are [mN m$^{-1}$].

| solvents | $\gamma^{d}$ | $\gamma^{p}$ | $\gamma^{total}$ |
|---|---|---|---|
| water | 21.8 | 51.0 | 72.8 |
| glycerol | 37.0 | 26.4 | 63.4 |

**Table S8.** Contact angles and surface tension of $P_D$s and Y6-BO, and the interfacial tension between $P_D$s and Y6-BO.

| Materials | Contact angle [deg] | | Surface tension [mN m$^{-1}$] | Blend systems | $\gamma^{D\text{-}A\ a)}$ [mN m$^{-1}$] |
|---|---|---|---|---|---|
| | water | Glycerol | | | |
| PM6 | 105.5±0.5 | 91.8±0.2 | 21.6 | PM6:Y6-BO | 0.93 |
| PM6-B10 | 102.9±0.7 | 89.1±0.4 | 22.7 | PM6-B10:Y6-BO | 0.46 |
| PM6-B20 | 102.3±0.3 | 88.2±0.4 | 23.3 | PM6-B20:Y6-BO | 0.43 |
| Y6-BO | 96.7±0.7 | 83.0±0.3 | 25.3 | – | |

[a)] The interfacial tension between the $P_D$s and $S_A$.

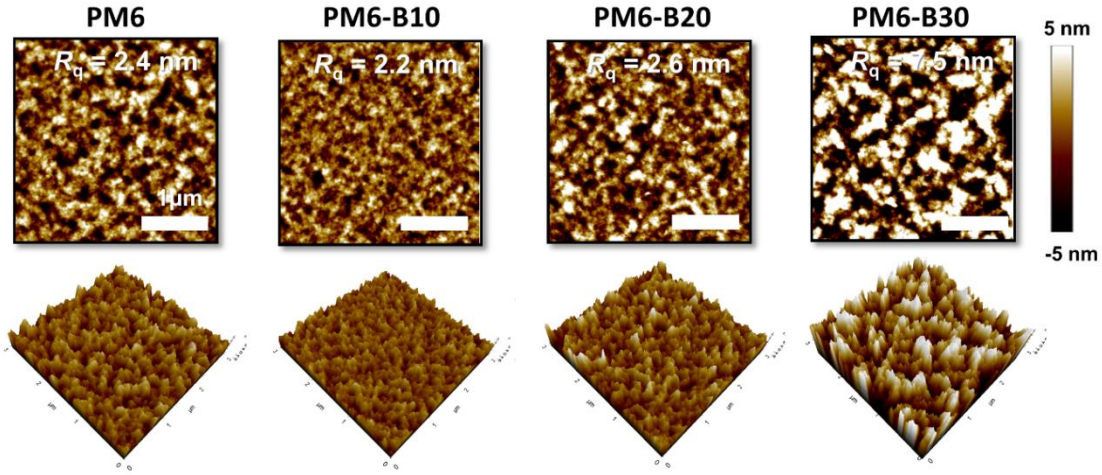


**Fig. S14.** AFM images of $P_D$:Y6-BO blend films.

**Table S9**. Mechanical properties of $P_D$ neat films and $P_D$:Y6-BO blend films.

| $P_D$s | Neat films | | | Blend films (*w* Y6-BO) | | |
|---|---|---|---|---|---|---|
| | $COS_{avg}$ [%] | Modulus (GPa) | Toughness (MJ $m^{-3}$) | $COS_{avg}$ [%] | Modulus (GPa) | Toughness (MJ $m^{-3}$) |
| PM6 | 14.9 ± 1.7 | 0.87 ± 0.04 | 3.5 ± 0.4 | 2.0 ± 0.5 | 1.36 ± 0.04 | 0.3 ± 0.1 |
| PM6-B10 | 23.8 ± 2.0 | 0.83 ± 0.04 | 5.9 ± 0.4 | 11.4 ± 0.5 | 1.19 ± 0.11 | 4.1 ± 0.4 |
| PM6-B20 | 22.7 ± 0.7 | 0.90 ± 0.05 | 5.5 ± 0.5 | 12.6 ± 0.8 | 1.91 ± 0.34 | 4.8 ± 0.8 |

## References


1. X. Cao, A. J. Miao, M. Zhu, C. Zhong, C. Yang, H. Wu, J. Qin and Y. Cao, *Chem. Mater.*, 2015, **27**, 96-104.
2. J. Yao, B. Qiu, Z.-G. Zhang, L. Xue, R. Wang, C. Zhang, S. Chen, Q. Zhou, C. Sun. C. Yang, M. Xiao, L. Meng and Y. Li, *Nat. Commun.*, 2020, **11**, 2726.
3. M. Zhang, X. Guo, W. Ma, H. Ade and J. Hou, *Adv. Mater.*, 2020, **11**, 4655-4660.
4. J. Comyn, *Int. J. Adhes.*, 1992, **12**, 145-149.
5. S. Wu, *J. Polym. Sci., Part C: Polym. Symp.*, 1971, **34**, 19-30.
6. E. Rynkowska, K. Fatyeyeva, S. Marais, J. Kujawa, W. Kujawski, *Polymers* 2019, **11**, 1799.